Macroscopic Traffic Flow Modelling

Editor: Victor L. Knoop

October 2017
Reader from and for graduate Students
Course by TRAIL research school

TU Delft

Preface

This books aims to explain the issues and recent advancements in macroscopic traffic modelling to (graduate) students. It is meant as follow-up material after a traffic flow theory course (for a book on that, see [19]). There are many scientific papers on this topic, which could be studied individually. The aim of this book is to make the papers more accessible, by ordering, explaining and giving examples.

This book contains the students' reports of the course Macroscopic Traffic Flow Modelling, which I lectured spring 2017 at the TU Delft. The chapters themselves are assignments by PhD students, bundeled by me.

Delft, October 2017

Contents

1

Traffic state dynamics in three representations

Maria J. Wierbos and Victor L. Knoop

1.1. Different representations

Traffic can be described by a fixed relation between X, N and T. The most common way to describe traffic is the N-model using Eulerian coordinates, which describes the number of vehicles (N) that have passed location x at time t. Another well-known representation is the X-model in Lagrangian coordinates, which describes the position (X) of vehicle n at time t. The third and least common representation is the T-model, which describes the time (T) at which vehicle n crosses location x ([23]). All three models describe the same traffic state, for example the situation shown in figure 1.1. The example displays the journey of around 75 vehicles on a single lane road. The 5th vehicle stops for around 60 timesteps and creates a jam, which slowly dissolves. With use of this example, the describing parameters, characteristics and shockwave theory in the 3 different approaches are described in the following sections.

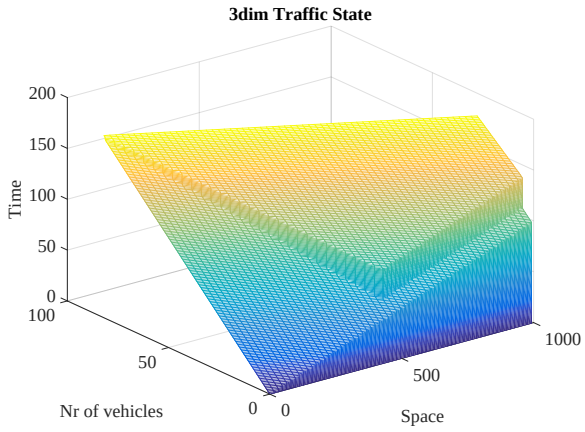

Figure 1.1: Example of a traffic situation, expressed in x, n and t

1.1.1. Describing parameters

In the different models, the traffic state are be explained in different combinations of x, n and t. The derivatives of these parameters give a first insight to the important variables. For example, the change in vehicle number n with time t is the flow q and the change of vehicle number n with space x is the density k. An overview of the other variables are presented in table 1.1. The pitfall in determining the derivatives are the correct signs, which originate from the convention of the scales. The convention of space can be either positive or negative, but time is

always positive. For vehicle number, the convention is that the first vehicle on a road has the lowest n number. As a result, the higher vehicle numbers correspond to lower x values, and the derivative dN/dx has a minus sign.

Table 1.1: Variables used in different coordinate systems

	$N(x,t)$	$X(n,t)$	$T(n,x)$
$/dt$	$q(x,t)$	$v(n,t)$	
$/dx$	$-k(x,t)$		$p(n,x)$
$/dn$		$-s(n,t)$	$h(n,x)$

1.2. Model characteristics

In this section the characteristics of the three models are described in more detail. The shape of the fundamental diagram is presented first, followed by the interpretation of trajectories, conservation equations and shockwave theory. For this sections, the based knowledge of traffic flow theory is assumed. Please look at the course reader of '*CIE 4821 Traffic Flow Theory and Simulation*' for further information.

1.2.1. N-model

The most common way to describe traffic is the N-model. In this model the flow q is proportional to the density k and speed u, with $q = ku$. A fundamental diagram can be drawn for flow where density is the main variable to determine the flow. Different shapes of the fundamental diagram are proposed to best capture the traffic behavior but for simplicity reasons only the triangular fundamental diagram is discussed here. The characteristics of the triangular fundamental diagram (Figure 1.2a) for flow as function of density $Q(k)$ are:

- Zero flow at jam density and zero density.
- A maximum flow value C when the density is at $k = k_c$
- A free flow branch for $0 < k \leq k_c$. In this range, flow increases linearly with density until it reaches the critical density k_c. The increase is equal to the free flow speed v_f.
- A congestion branch when density exceeds the critical density $k > k_c$. In this range, flow decreases with wave speed $-w$ until the density reaches jam density k_j

Trajectories in the N-model are iso-n lines which represent the movement of an individual vehicle in time and space. The XT-diagram in Figure 1.2b shows model output of around 75 vehicles driving on a 1 lane road, which is the same situation as in Figure 1.1. The 5th vehicle stops at $x = 450$ for around 60 timesteps, causing a jam. The trajectories of 3 cars are isolated, the first having an undisturbed path, the second trajectory is stationary for around 40 timesteps before continuing its path, and the third trajectory is stationary at a smaller x-location for a shorter time period. This indicates that the jam grows in the $-x$ direction, and that the queue length dissolves with time. In this model data, but also in observed trajectory data, the vertical distance between two trajectories provides information about the density, using $\frac{\Delta x}{\Delta N} = -\frac{1}{k}$. The horizontal distance between trajectories is a measure for the flow $\frac{\Delta t}{\Delta N} = \frac{1}{q}$.

Assuming that all vehicles that enter a certain road stretch also have to exit the road stretch within a certain amount of time, it can be stated that the number of vehicles are conserved. The conservation equation is given by:

$$\frac{\delta k}{\delta t} + \frac{\delta q}{\delta x} = 0$$

which states that the change in density k with time t and the change of flow q with distance x should equal out to zero.

Shockwave Theory in the XT-plane

By combining trajectory data and the fundamental diagram, it is possible to identify traffic states. These traffic states are a combination of density and flow, for example, jam state or capacity state. Figure 1.3 shows an example the traffic states which are identified using the fundamental diagram.

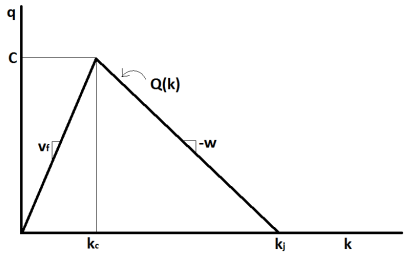

(a) Fundamental diagram for the N-model

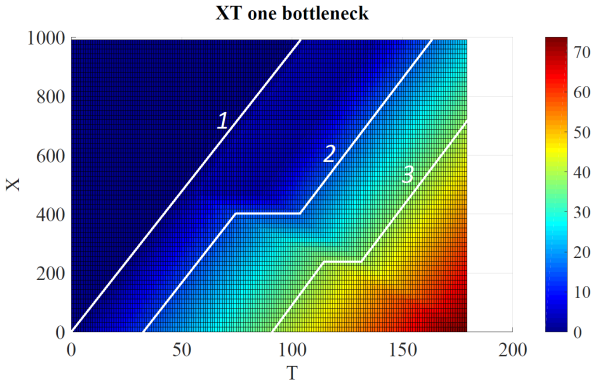

(b) XT-diagram and iso-n lines, with 3 trajectories. The colors indicate the vehicle number.

Figure 1.2: Representation of traffic in the N-model

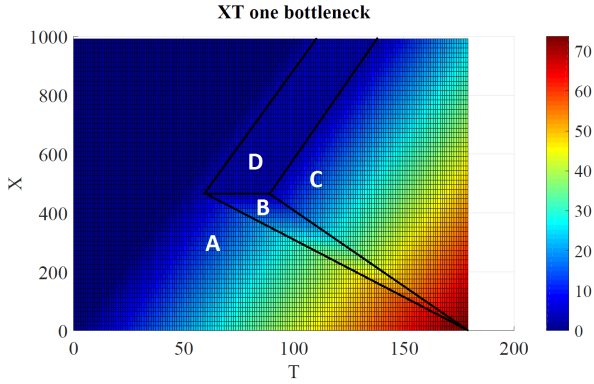

(a) XT-diagram with different traffic states

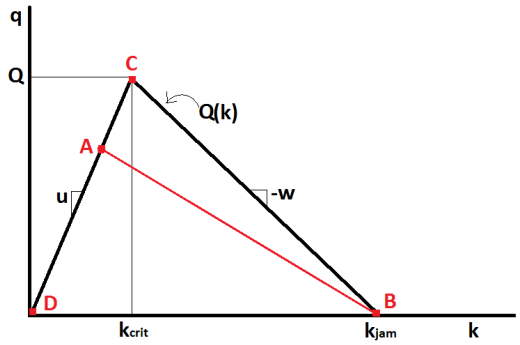

(b) Fundamental diagram with different traffic states

Figure 1.3: Shockwave Theory in the N-model, with different traffic states, A = inflow, B = jam, C = Capacity, D = empty road

1.2.2. X-model

In the X-model, the fundamental diagram describes the speed V based on the spacing s. The shape of $V(s)$ is presented in Figure 1.4a and has the following characteristics:

- A speed of 0 between the origin $s = 0$ and the jam spacing s_j
- A congestion branch where speed increases with spacing. This state occurs when $s_j < s \leq s_c$, the angle of increase is equal to $\tau = 1/(wk)$
- A free flow branch where the speed is maximum and continuous (v_f). This state occurs when spacing exceeds the critical value $s > s_c$
- A critical spacing s_c which is the minimum value for spacing with maximum speed (v_f)

From the perspective of the X-model, the traffic situation of Figure 1.1 is visualized in the NT diagram 1.4b. Looking horizontally in the plot, there is a continuous increase in distance (colors) for the first vehicles, indicating that they have an undisturbed journey. Vehicle nr 20 is positioned on 1 location for a period of time, so it experiences a delay due to a jam. The length of the jam is not visible in this representation, only the delay it causes. The delay is largest for the lower vehicle numbers (but >5) and decreases with time for higher vehicle numbers, indicating that the jam is slowly dissolving. Furthermore, the delay starts at a distance around 400m (green color) and changes to blue colors with time, indicating that the jam is moving in the $-x$ direction.

Trajectories in the X-model are iso-x lines. It tracks how many vehicles have crossed a fixed location with time, in other words, every trajectory is cumulative curve. The three indicated trajectories in Figure 1.4b are cumulative curves for approximately $x = 100, x = 400$ and $x = 600$.

From the NX diagram, also other traffic variables can be estimated. The vertical distance between two trajectories is a measure for density $\frac{\Delta n}{\Delta X} = -k = -\frac{1}{s}$ and the horizontal distance can be used to estimate the pace $\frac{\Delta t}{\Delta X} = p = \frac{1}{v}$.

Based on the assumption that vehicles cannot disappear from the road, a continuity equation can be retrieved. The continuity equation for the X-model is:

$$\frac{\delta s}{\delta t} + \frac{\delta v}{\delta n} = 0$$

which states that the change in spacing s with time t and the change of speed v with vehicle number n should equal out to zero.

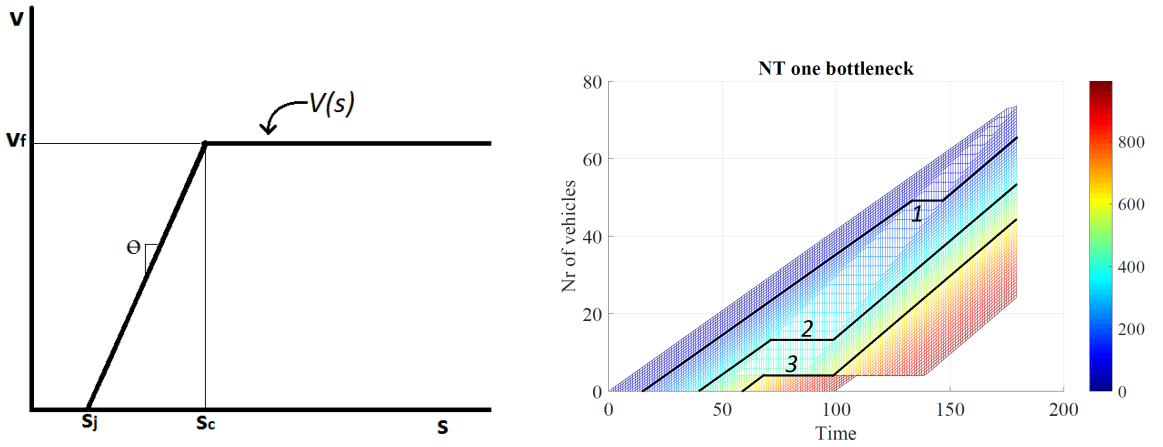

(a) Fundamental diagram for the X-model

(b) NT-diagram and iso-x lines, with 3 trajectories. The colors indicate the location x.

Figure 1.4: Representation of traffic in the X-model

Shockwave Theory in the NT plane

Similar to Shockwave Theory in the N-model, it is possible to also identify traffic states in the X-model. This is done by combining the trajectory data in the NT-plane with the fundamental diagram, as shown in Figure 1.5. Four states can be identified: Inflow A, jam B, capacity C and empty road D. The steps to identify traffic states is similar to the shockwave theory in the XT-plane, with 1 exception. The spacing on an empty road can be infinitely large, so state D does not have an exact position in the fundamental diagram. Since the spacing at D is infinitely large, the shock between jam B and empty road D is horizontal in the limit. Furthermore, the size of the shock is infinitely small, so it is invisible in the NT-diagram. The connecting line between inflow state A and jam state B, indicates how fast the jam is growing, whereas the connection line between jam state B and capacity state C, gives information on how the jam dissolves.

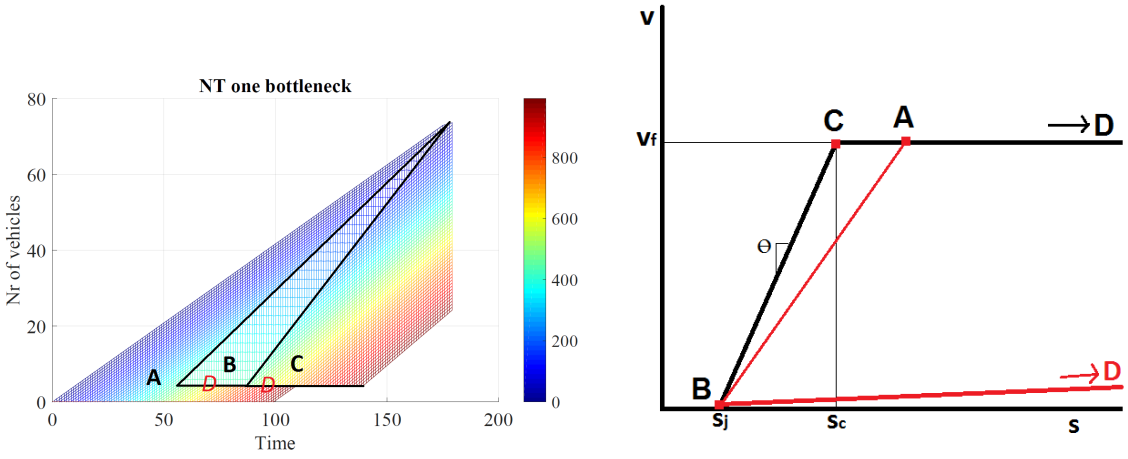

(a) NT-diagram with different traffic states

(b) Fundamental diagram with different traffic states

Figure 1.5: Shockwave Theory in the X-model, with different traffic states, A = inflow, B = jam, C = Capacity, D = empty road. Traffic state D is infinitely small.

1.2.3. T-model

The variables used to describe traffic states in the T-model are pace p and headway h. The characteristics of the fundamental diagram for headway as function of pace $H(p)$ are:

- There is a capacity state at a minimum pace p_c where headway is minimum H_c at $H = 1/C$
- Headway increases from H_c to infinity in the free flow branch, so it is a vertical line at $p = 1/v_f$
- Headway increases with pace in the congested branch with angle ϵ which equals $1/k_j$
- For high values of pace (=low speed), the headway increases to infinity

The traffic state in the T-model is represented in the NX-plane, see Figure 1.6. In this graph, the colors represent the time, so a jump in coloring indicates the boundary to a different traffic state. A horizontal line in the NX diagram gives the time at which all vehicles cross a certain location, so the vertical color jump indicates that there is an empty road. A vertical line in the NX diagram follows 1 vehicles and give the time at which that vehicle passes a certain position. The color jump in vertical direction indicates that the vehicle takes a longer time than usual before reaching the next position, so it is caught in a jam. The extent of the color jump indicates the magnitude of the jam. A large jump equals a large delay.

Trajectories in the T-model are iso-t lines which are basically snapshots. It provides the position of all vehicles on the road at a certain time step. The orientation of the line is from the upper left to the lower right, which is opposite to the trajectories in the other two models. The different orientation is a result of the convention of scale in vehicle number, as mentioned in section 1.1.1. The example trajectory nr 2 in Figure 1.6b indicates that the first 5 vehicles are situated around 800 distance, followed by an empty road. Then, approximately 5 vehicles are going at capacity flow between 550 to 450 distance, while 10 vehicles are trapped in a jam around distance 400. Finally, 10 vehicles are situated between distance 0 and 375 in the 'normal' or initial traffic state. It is difficult to see in this example, but the slope of trajectory is smallest (least negative) in the capacity state. In general, the vertical distance between two trajectories is an estimation of speed $\frac{\Delta x}{\Delta T} = v = \frac{1}{p}$ while the horizontal distance is a measure for the flow $\frac{\Delta n}{\Delta T} = q = \frac{1}{h}$.

Assuming that no vehicles disappear from the road, the continuity equation for the T-model is given by:

$$\frac{\delta p}{\delta n} - \frac{\delta h}{\delta x} = 0$$

stating that the change of pace p with vehicle number n should be equal to the change in headway h with distance x.

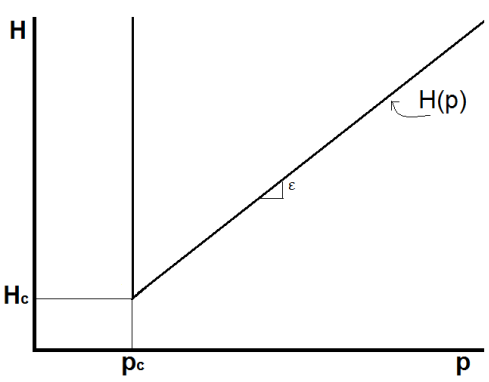

(a) Fundamental diagram for the T-model

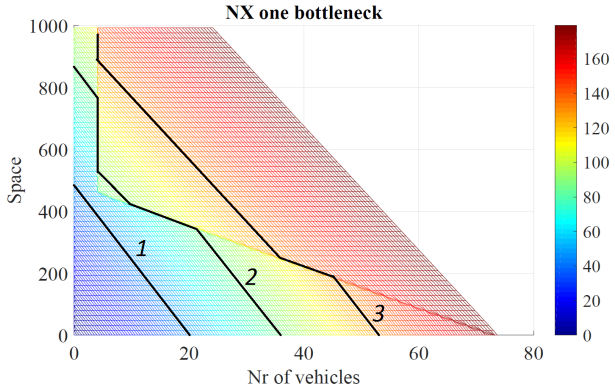

(b) XN-diagram and iso-t lines, with 3 trajectories. The colors indicate the time.

Figure 1.6: Representation of traffic in the T-model

Shockwave Theory in the NX-plane

Due to the opposite orientation of the trajectories, the fundamental diagram needs to be adjusted before shockwave theory can be applied. Since the free flow branch of the $H(p)$ is vertical, it is sufficient to only reflect the congested branch in the line $H = H_c$, resulting in a line with angle $-q$. This line is partially drawn in Figure 1.7b, with jam state B' located at minus infinity.

Returning to the XN-diagram, two traffic states are easily recognized due to the jumps in color, with initial state A in the lower part and the capacity state C in the upper right part. In between these states, two infinitely small traffic states exists. State D indicates the empty road, and state B indicates the jam state. The headway for an empty road and at stand still are both infinitely large, therefore the states B and D are not physical points in the fundamental diagram, but indicated with the arrows. Because the jam state is infinitely large, the shockwave of the jam (B) with the inflow (A) and outflow (C) are parallel, with an infinitely small area in between. A similar reasoning holds for the empty road state D, which is situated in between the initial state A and capacity state C.

Only the tail of the queue is visualized in the NX-diagram, and not the queue itself. This is because stopped vehicles do not move in X and therefore are not visualized. Only in the time step where they start to move again, the vehicles are visualized in the next state. The tail of the jam moves in $-x$ direction with slope $-\epsilon = -\frac{1}{k_j}$, so it depends on the jam density only. In this example, the tail of the jam grows till it reaches the beginning of the road. If the jam had dissolved sooner, there would have been another vertical shock between capacity state C and inflow state A, at the vehicle number that does not experience any delay anymore.

Although shockwave theory can be applied in this representation, it does not provide extra information. The occurrence of a jam can be identified from this graph and the growth of the jam in space can be estimated. However, it is impossible to identify when the congestion will be dissolved. This is a disadvantage of this representation.

1.3. Summary

In summary, the N-model is more intuitive and easy to understand. The X-model is mathematically easier but more difficult to interpret. The X-model is difficult to grasp and does not yet have clear benefits. Table 1.2 provides an overview of the main parameters used in the different representation.

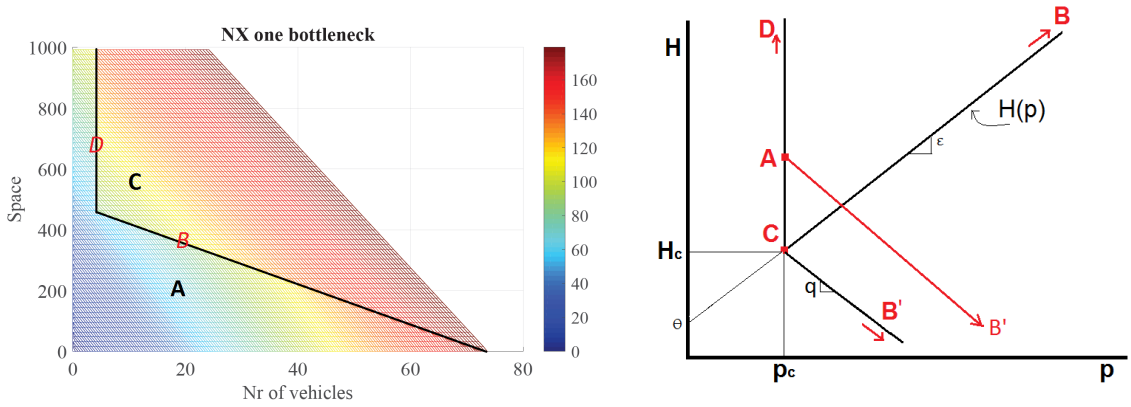

(a) XN-diagram with different traffic states

(b) Fundamental diagram with different traffic states

Figure 1.7: Shockwave Theory in the T-model, with different traffic states, A = inflow, B = jam, C = Capacity, D = empty road. Traffic state B and D are infinitely small.

Table 1.2: Overview of parameters

	$N(x,t)$	$X(n,t)$	$T(n,x)$
1st explanatory variable	x	n	n
2nd explanatory variable	t	t	x
Independent variable	$-k$	$-s$	p
Dependent variable	q	v	h
FD	$Q(k)$	$V(s)$	$H(p)$
Trajectories	iso-n	iso-x	iso-t
slope trajectories	$\frac{dx}{dt} = v$	$\frac{dn}{dt} = q$	$\frac{dx}{dn} = -s$
vertical distance	$\frac{\Delta x}{\Delta N} = -\frac{1}{k}$	$\frac{\Delta n}{\Delta X} = -k$	$\frac{\Delta x}{\Delta T} = v$
horizontal distance	$\frac{\Delta t}{\Delta N} = \frac{1}{q}$	$\frac{\Delta t}{\Delta X} = p$	$\frac{\Delta n}{\Delta T} = q$

2

Variational theory

Boudewijn Zwaal

2.1. Introduction

The variational principle of traffic flow theory is an analytical method to determine the capacity of a road. This works as follows. An observer of the road may experience a flow given the current traffic conditions. This observer might be moving along the road for a given time, which influences the flow he observes. Of course, there are traffic conditions that will lead to the highest flow possible to observe for this observer. This is thus an upper bound to the flow: it cannot get any higher than this. The path of this observer however, may increase of decrease this value. The path that leads to the lowest upper bound then is the capacity of the road. There is no higher flow possible. The goal is therefore to find this path of the moving observer.

2.2. Mathematical formulation

2.2.1. Derivation of the traffic flow model

In this section we will derive the mathematical formulation of variational theory. For an example we refer to section 2.3. Variational theory uses kinematic wave theory. In the kinematic wave theory we model the cumulative number of vehicles at a certain location and time, $N(t,x)$. Hereby, we assume that this function $N \in \mathscr{C}^2$ almost everywhere[1], i.e., it is almost everywhere continuously differentiable up until at least the second derivatives. The model is then entirely given by the following partial differential equation

$$\frac{\partial N}{\partial t} = Q(-\frac{\partial N}{\partial x}), \tag{2.1}$$

where Q is the Fundamental Diagram of traffic flow. We use the following notation $\frac{\partial N}{\partial t} = q$ and $-\frac{\partial N}{\partial x} = k$, respectively the flow and the density, to obtain

$$q(x,t) = Q(k(x,t)). \tag{2.2}$$

We can use the property that N is twice continuously differentiable almost everywhere to state that $\frac{\partial^2 N}{\partial x \partial t} = \frac{\partial^2 N}{\partial t \partial x}$, which is equivalent to

$$\frac{\partial k}{\partial t} + \frac{\partial q}{\partial x} = 0, \tag{2.3}$$

which shows conservation of the quantity N (conservation of mass) on the domain.
Some more definitions are needed. The solution $N(t,x)$ of (2.1) is an almost everywhere differentiable surface $\mathscr{D} \subset \mathbb{R}^3$ whose projection onto $\mathbb{R}^2$, or the x-t plane (we will use $D \subset \mathbb{R}^2$ as notation for the domain), are the so called characteristic lines of equal N. A path $\mathscr{P}$ in the x-t plane is defined as a continuous and piecewise differentiable function $x(t)$. For the remainder of this chapter we need all paths to originate from the boundary ∂D and we

[1] Almost everywhere means everywhere in the domain except on a subset of measure zero (which are the shocks), see chapter 3 of [9] for an analytical background on shock waves.

therefore define the set V_P to be the set of all paths originating at the boundary and ending in a point P.
At any point (t, x) within D the rate of change of N is given by

$$\frac{dN}{dt} = \frac{\partial N}{\partial t} + \frac{\partial N}{\partial x}\frac{\partial x}{\partial t} = q - ku, \tag{2.4}$$

where we used the chain rule. Here, u can be interpreted as the speed of a moving observer. Formally, the change in N between two points t_1 and t_2 can be computed by taking the integral of equation (2.4) (note we use $q = Q(k)$)

$$N_{t_2} - N_{t_1} = \int_{t_1}^{t_2} Q(k) - ku\, dt, \tag{2.5}$$

where the integral is computed along the path $\mathscr{P} = x(t)$ between t_1 and t_2 where a moving observer travels with speed $u(t)$. Note that for a given solution $N(t, x)$ this value is invariant of the chosen path $\mathscr{P}$ (because N is a conserved quantity).

2.2.2. Variational theory

Equation (2.5) gave us an expression for the change in cumulative vehicle number between any two points given the traffic conditions (i.e., given the solution $N(t, x)$). To find the capacity of a certain road, we need to have the lowest upper bound of this change in vehicle number, i.e., the lowest upper bound of the flow. For a given path the upper bound to (2.5) is given by

$$N_{t_2} - N_{t_1} \leq \int_{t_1}^{t_2} \max_k\{Q(k) - ku\}\, dt.^2 \tag{2.6}$$

Note that a given k along the path fixes the values of Q along the path and that the speed of the moving observer is fixed by the chosen path. Therefore this is a optimisation problem in one variable. Let us define for a given path $\mathscr{P} \in V_P$ that $R(k) := \max_k\{Q(k) - ku\}$ and

$$\Delta\mathscr{P} = \int_{t_{\partial D}}^{t_P} R(k)\, dt. \tag{2.7}$$

This then proves the following theorem[3].

Theorem 1. *Let $B \in \partial D$ be a point on the boundary of the domain and $P \in D \setminus \partial D$ a point in the interior of the domain. Then for any solution $N(t, x)$ of (2.1) the change in cumulative vehicle numbers is bounded from above, i.e., $N_P - N_B \leq \Delta\mathscr{P}$ for any path $\mathscr{P} \in V_P$ from B to P.*

This implies that any path gives an upper bound to the change in cumulative vehicle number. In other words, the lowest upper bound gives the maximal flow possible. This allows us to establish the formula which forms the basis of variational theory:

$$N_P = \min_{\mathscr{P}}\{B_{\mathscr{P}} + \Delta\mathscr{P} : \forall\mathscr{P} \in V_P\}.^4 \tag{2.8}$$

Here $B_{\mathscr{P}}$ is the beginning of the path (on the boundary of the domain).

2.3. Applicability of variational theory

So the goal is now to find this path $\mathscr{P}$ for which the observed flow is minimal. To find the actual capacity of the road, the one requirement is that we start and end at the same value for x. There are a number of tricks to find this shortest path, so let us first look at a typical x-t plane of a single lane road with one traffic light (fig. 2.1) and the Fundamental Diagram $Q(k)$ for this road (fig. 2.2). This traffic light has 60 s green time and 60 s red time.

It has been shown in [6] that it always gives a shorter path to move at the two extremes of possible observer speeds (which are determined by $\frac{dQ}{dk}$, the slope of the FD). In our case, this means at free flow speed and at wave speed. Now, finding the capacity of a road means we may assume vehicles driving at capacity (i.e. $q_{\max}$) and thus at free flow speed. So a moving observer moving at free flow speed too will not observe any flows. Then, we have the red phase of the traffic light. Obviously there will be no flow through the red phase, which means that this

[2] Don't be confused that [5] uses the supremum in this formula, which is because he develops the theory for arbitrary $k \in \mathbb{R}$. Since for traffic $k \in [0, k_{\text{jam}}]$, the set $\{Q(k) - ku\}$ is compact (Q is continuous) and therefore the supremum equals the maximum.

[3] Part of this proof is omitted for readability. However, it is important to note that for this proof we need the assumption that Q is concave, which in the case of traffic is obviously reasonable.

[4] The ambitious reader is challenged to prove that this set is indeed compact and the minimum exists.

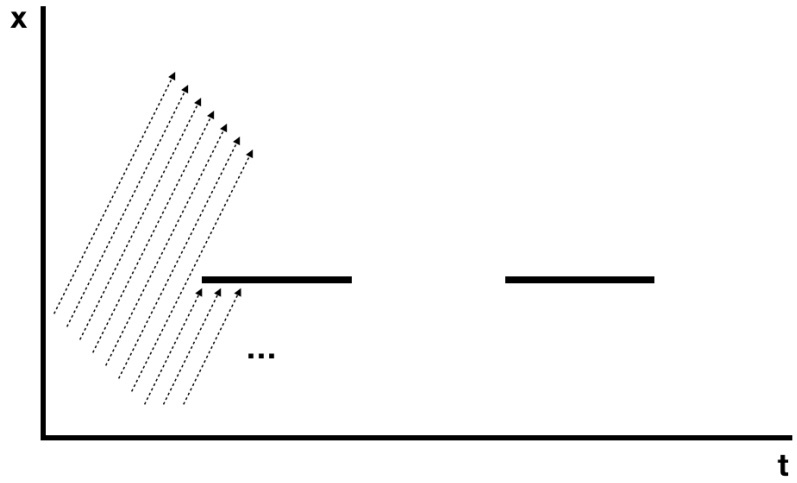

Figure 2.1: x-t plane of the road with one traffic light.

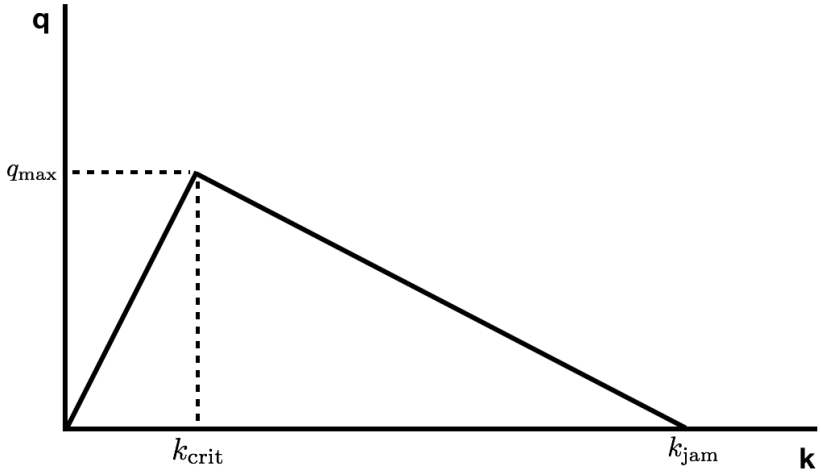

Figure 2.2: The FD of the road.

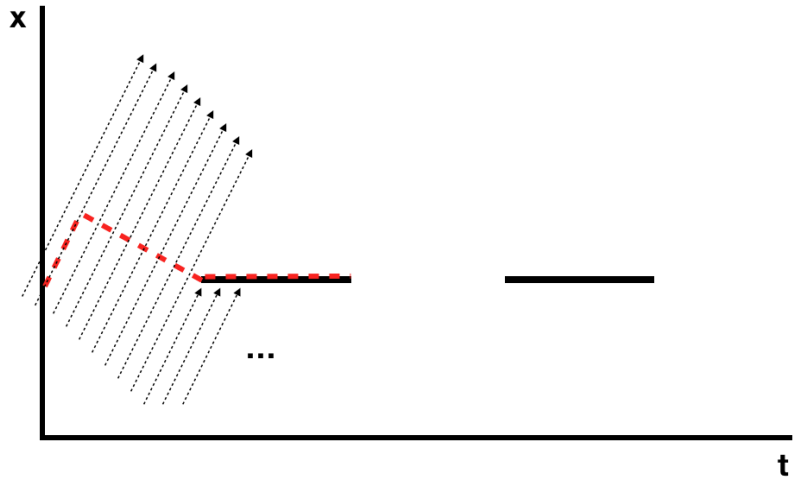

Figure 2.3: The shortest path.

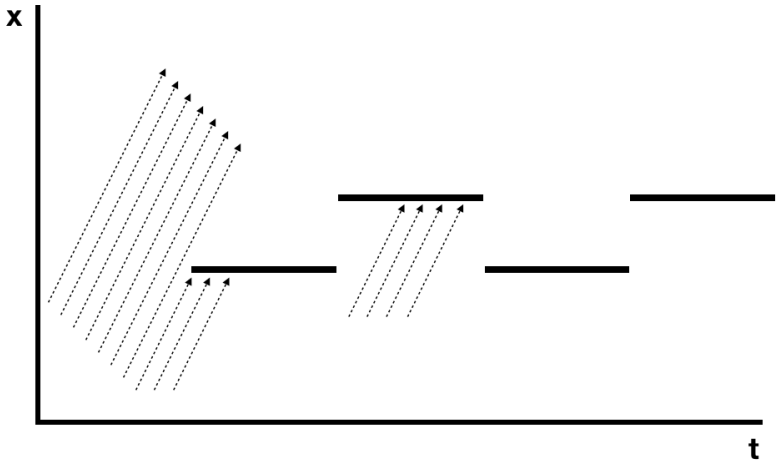

Figure 2.4: Situation with two traffic lights.

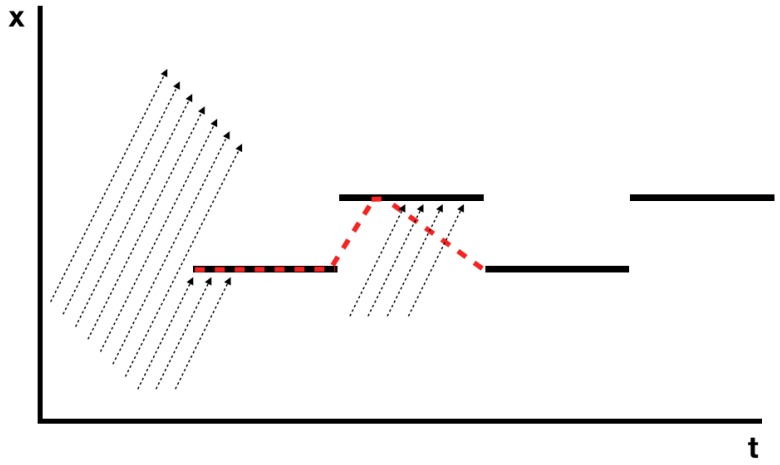

Figure 2.5: One of the shortest paths.

is very efficient to include in the path of the moving observer (recall we are looking for the shortest path). Then finally, moving at the wavespeed backwards means we encounter the maximal flow, $q_{\max}$. As a final remark, note that we *should* compute the flow for all $t \in [0, \infty]$, however, in this case we can make use of the periodicity of the traffic light smartly. For the shortest path, see figure 2.3

Now the capacity of the road is easily calculated. Of the shortest path, only during $\frac{k_{\text{jam}} - k_{\text{crit}}}{k_{\text{jam}}}$ of the green period of 60 seconds a flow is measured, which is $q_{\max}$. Making use of the periodicity we divide by 120 seconds for the full cycle to obtain a capacity of

$$C = q_{\max} \frac{k_{\text{jam}} - k_{\text{crit}}}{k_{\text{jam}}} \frac{60}{120}. \tag{2.9}$$

The idea of describing the problem of finding the road capacity as a shortest-path algorithm can be applied to a situation with two traffic lights as follows. Consider the situation as described in figure 2.4. The traffic lights are a km apart, both the green and red time are 60 seconds and the offset is 60 seconds as well.

Here, we can also make use of the periodicity of the situation. Of course, we want to use as much of the red phases as possible. Since can travel forward with the free flow speed and backwards with the wave speed, we have more possibilities that give the same cost. In fact, like the previous example, the only cost we will make is during the backwards travelling, as can be seen in figure 2.5. Travelling from the downstream traffic light to the upstream traffic light with the wavespeed will take $\frac{a(k_{\text{jam}} - k_{\text{crit}})}{q_{\max}}$ hours. Since the situation is periodic for 120 seconds again,

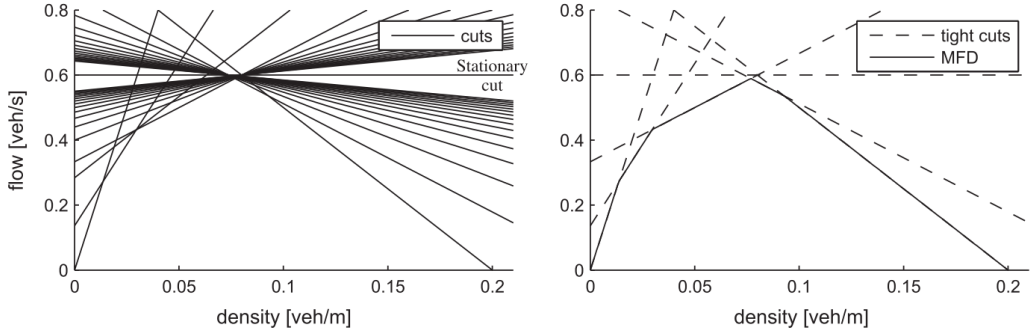

Figure 2.6: The MFD is the minimum of all lines defined by the shortest path for a given average speed of the moving observer.

we get the final answer (in veh/h) as

$$C = q_{\max} \frac{a(k_{\text{jam}} - k_{\text{crit}})}{\frac{120}{3600} \cdot q_{\max}} = \frac{3600a(k_{\text{jam}} - k_{\text{crit}})}{120} = 30a(k_{\text{jam}} - k_{\text{crit}}). \tag{2.10}$$

So in short:

- To find the shortest path, we move at free flow speed or wave speed through the x-t plane.
- We use as many bottlenecks as possible (moving bottlenecks too) since the flow through them is either zero or decreased.
- We make use of periodicity whenever possible for easier calculations.
- This problem gets complicated extremely quickly and solving by hand is almost always impossible; instead we rely on shortest path algorithms.

2.4. Variational theory to estimate MFDs

In the previous section, we estimated the capacity of a road stretch. Notice that the average speed of the moving observer is zero in this case, since he begins and ends at the same x. If we now want to estimate an MFD of a certain road stretch (for the theoretical background on MFDs see chapter ??), we can use the following expression

$$Q(k) = \inf_u \{ku + R(u)\}, \tag{2.11}$$

where

$$R(u) = \inf\{B_{\mathscr{P}} + \Delta\mathscr{P}(u) : \forall \mathscr{P} \in V_P\} \tag{2.12}$$

with u being the average speed of the moving observer. Proof of (2.11) can be found in [7]. An intuitive visualization is shown in figure 2.6.

2.5. Variational theory to get a lower bound for the capacity

Consider a situation as shown in figure 2.7. One can determine an upper bound using variational theory as described up to now. A lower bound can also be found, which has been investigated by [8]. They state that the cost of a feasible path is given by

$$C = \frac{\sum_i L_i}{\sum_i L_i + \sum_i O_i}. \tag{2.13}$$

Here L_i is the duration of a segment to another bottleneck and O_i is the time spend at a bottleneck. Now given their parameters they can say that O_i is at most 1 and thus that the upper bound for O_i is 1. Also, the least amount

of time spend between two bottlenecks is some value M_i in their simulation and this is therefore a lower bound for L_i. This way, we know for sure that

$$\frac{\sum_i M_i}{\sum_i M_i + \sum_i 1} \leq \frac{\sum_i L_i}{\sum_i L_i + \sum_i O_i}, \tag{2.14}$$

and we have our lower bound for the flow.

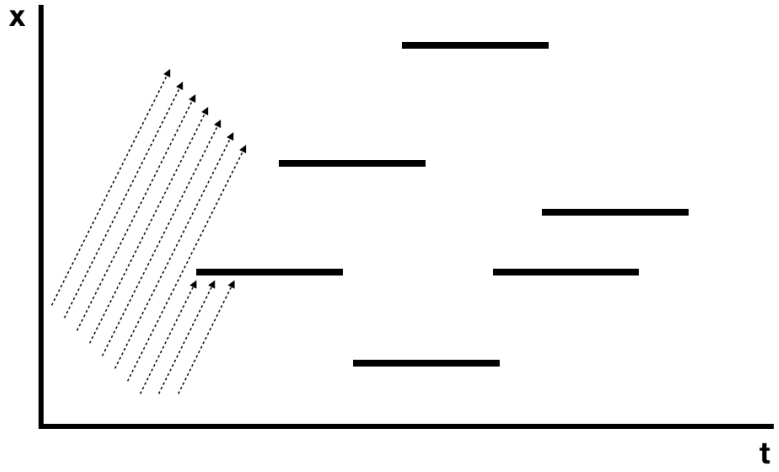

Figure 2.7: Random static bottlenecks (for instance crossing pedestrians).

3

The Lagrangian Coordinate

Tin T. Nguyen

Preface

This document provides a general introduction to traffic flow in the Lagrangian coordinates. Some remarks on LWR model in this coordinates system are also provided. This is done based on the following materials:

- The Lagrangian coordinates and what it means for first order traffic flow models [24].
- TRAIL (the Netherlands Research School for Transportation, Infrastructure and Logistics) course: Macroscopic Traffic Modeling [20].

3.1. Introduction

The Lagrangian coordinates system is one of the two common coordinate systems, the other one is Eulerian, in the field of fluid dynamic. When applying to traffic flow, they can be intepreted as follows.

- Eulerian coordinates system is to observe traffic flow at a specific location. Therefore, the representative function is counts of vehicles (N) passing the location (x) over time (t), i.e. function $N(x,t)$.
- Lagrangian coordinates system is intepreted as moving with traffic flow. It means to record locations (X) of vehicles (n) over time (t). Consequently, the representative function is $X(n,t)$.

Table 3.1 summarizes some underlying features in the two coordinate systems. The main variable of traffic flow in Lagrangian coordinates is spacing (s), which can be understood as the distance between vehicles. It is also the inversion of density, which is the main variable in Eulerian coordinates. The next important quantity is flux which is represented by speed in Lagrangian coordinates. Consequently, the fundamental relation of traffic flow in the Lagrangian is the relation between the flux and the main variable, i.e. $V^*(s)$. This will be elaborated more in the next section of the document.

Table 3.1: A comparision of Eulerian and Lagrangian Coordinates - Table 1 [24]

	Eulerian coordinates	**Lagrangian coordinates**
Unknown function	N	X
Main variable	$k = -\frac{\partial N}{\partial x}$	$s = -\frac{\partial X}{\partial n}$
Flux	$q = \frac{\partial N}{\partial t}$	$v = \frac{\partial X}{\partial t}$
FD	$Q(k)$	$V^*(s)$

$*$ Some conventions and remarks

- Vehicles are numbered in reverse order to driving direction as shown in figure 3.1.

- Locations are marked in an increasing order according to driving direction (see figure 3.1).
- As n increases, X decreases. This explains the negative sign in the calculating equation of spacing in table 3.1.
- Given a vehicle, as time passes by (i.e. increases), its location increases. Therefore, the sign of right hand side (RHS) of the calculating equation of speed is positive (see table 3.1).

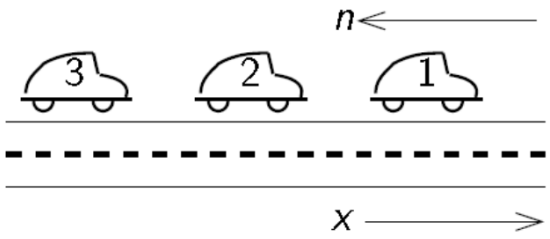

Figure 3.1: Numbering vehicles [20]

3.2. Lagrangian conservation law

Similar to vehicle conservation in Eulerian coordinates, there is an equivalent equation in Lagrangian coordinates. This time, we will consider the conservation of distance. In partically, taken the length of a platoon of dn vehicles, the following relation always holds [20]:
length_new = length_old + distance travelled by the first vehicle - distance travelled by the last vehicle
Hence,

$$s_{new} * dn = s_{old} * dn + v_{first} * dt - v_{last} * dt$$

$$\frac{ds}{dt} + \frac{dv}{dn} = 0 \tag{3.1}$$

For a visuallization of this calculation, see figure 3.2.

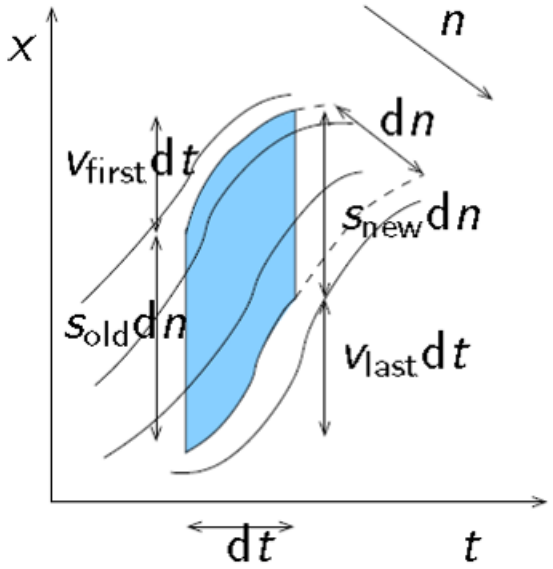

Figure 3.2: Interpretation of calculating platoon length - [20]

3.3. LWR model in Lagrangian Coordinates

This section presents some main concepts related to LWR model in Lagrangian coordinates. They cover fundamental diagram and numerical solution.

3.3.1. Fundamental diagram

Traffic represented in Lagrangian coordinates, similarly to Eulerian coordinates, also has a fundamental diagram which describes the relation V^* between v and s (as mentioned in previous section). This can be done simply by combining the fundamental diagram $Q(k)$ with the following features:

- $s = 1/k$
- $v = q/k$

Figure 3.3(a) and 3.3(b) depict the fundamental relations in the Eulerian and Lagrangian coordinates systems respectively. We can simply divide traffic into two general states: free flow and congestion. Accordingly, two remarks for the relation $V^*(s)$ are as follows.

- In free flow, speed is constant (v_m) which is represented by the RHS part of the diagram ($s > s_c$). This is equivalent to the LHS part of the diagram in Eulerian coordinates.
- In congestion, the LHS part, from right to left, the spacing is decreasing until it reaches minimum value which will be in the case of traffic jam. Accordingly, the speed is reducing linearly until zero.

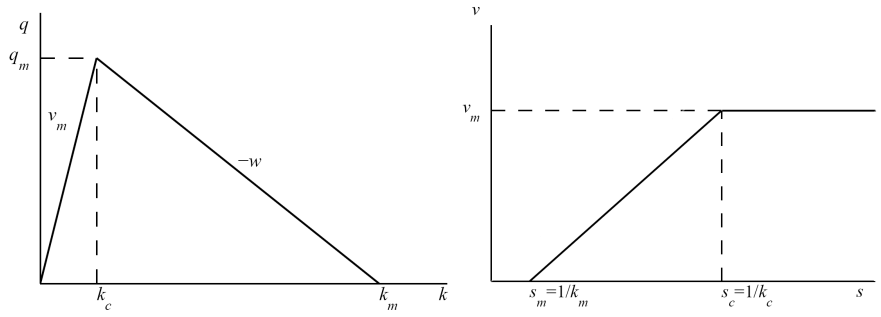

(a) In Eulerian coordinates (b) In Lagrangian coordinates

Figure 3.3: Fundamental diagrams - Figure 2 [24]

3.3.2. Numerical solution

Gudonov scheme [12] is used to discretize the equation 3.1. The n-axis is divided into cells with size of Δn. This means each cell comprises of Δn vehicles and the spacing (s) between them is updated every time step Δt.

Recall LWR model in Eulerian coordinates, Gudonov scheme needs to introduce the Demand-Supply formula to solve the problem in which traffic information can propagate in different directions under different conditions. This is coherent with the fundamental diagram shown in figure 3.3(a). The relation function $Q(k)$ changes direction when it crosses critical density.

This problem can be avoided when working in Lagrangian coordinates. As it is shown clearly in figure 3.3(b), the relation function $V^*(s)$ is a monotonic function. Therefore, traffic information only moves in one direction which makes it easier to compute numerically in Lagrangian coordinates. Equation 3.2 (Equation 10 - [24]) shows the update of cell spacing over time.

$$s_i^{t+\Delta t} = s_i^t + \frac{\Delta t}{\Delta n}(V^*(s_i^t) - V^*(s_{i-1}^t)) \tag{3.2}$$

4

Second-order traffic flow models

P.B.C. van Erp

4.1. Introduction

In this report, we will limit ourselves to general understanding the models. For additional information and mathematical insights the reader is referred to the papers cited in this report.

Over sixty years ago, [38] proved the basic relation between the three macroscopic variables flow q, density k and speed u. They showed that $q = ku$. This relation in combination with the physical condition of the conservation of vehicles is important for any macroscopic traffic flow model. For a road segments without discontinuities, e.g., ramps, this conservation of vehicles can be written as a Partial Differential Equation (PDE):

$$\partial_t k + \partial_x q = 0 \tag{4.1}$$

4.2. The first-order LWR-model

[26] and [33] independently showed the fundamental relation between the macroscopic variables, which is now known as the fundamental diagram. They showed that q can be expressed as a function of k and correspondingly u as a function of k, i.e., $V(k)$. Incorporating the speed-density relation in the conservation of vehicles yields the LWR-model:

$$\partial_t k + \partial_x (kV(k)) = 0 \tag{4.2}$$

The LWR-model combines the conservation of vehicles with a fundamental diagram. This diagram describes the traffic in equilibrium states [17]. Therefore, the LWR-model is restricted to these equilibrium states. However, in reality, traffic is often observed in non-equilibrium. For example, transitions from one state to the other, e.g., from a free-flow state to a congested state, are not instantaneous. In the LWR-model, these transitions between states, i.e., shocks, are too coarse [3]. Furthermore, Daganzo discusses two other deficiencies of the LWR theory: *its failure to describe platoon diffusion properly (a phenomenon that takes place over long distances and times when traffic is light; ...) and its inability to explain the instability of heavy traffic, which exhibits oscillatory phenomena on the order of minutes.*

4.3. Second-order traffic flow models

To describe non-equilibrium states, we can use second- or higher-order traffic flow models. Such models use extra partial differential equations which opt to correctly describe the macroscopic traffic behavior.

[32] and [39] proposed a second-order traffic flow model which incorporates a momentum (dynamic velocity) equation:

$$\partial_t u + u\partial_x u + k^{-1} p'(k)\partial_x k = \left(\tau^{-1}\right)(V(k) - u) + \nu\partial_x^2 u \tag{4.3}$$

This momentum equation involves a pressure term $p(k)$ and two parameters, i.e., τ and ν. It is important to note that adding additional parameters requires additional calibration, which may lead to practical challenges.

[3] shows that these higher-order modifications, i.e., the momentum equation, have physical limitations. He argues that their basis, i.e., fluid/gas dynamics, do not fully apply to traffic dynamics. Here, he denotes three essential differences between the two (this summation is copied from [3]):

1. *A fluid particle responds to stimuli from the front and from behind, but a car is an anisotropic particle that mostly responds to frontal stimuli,*
2. *The width of a traffic shock only encompasses a few vehicles, and*
3. *Unlike molecules, vehicles have personalities (e.g., aggressive and timid) that remain unchanged by motion.*

The first point addresses the anisotropic characteristics of vehicles. Anisotropic means that a physical property differs in direction of measurement. For instance, in the PW-model, the change in u over t, i.e., acceleration, depends on the difference in k over x. A positive difference in k over x, i.e., k is larger in downstream than in upstream direction, has a negative influence on the acceleration. [3] argues (correctly) that vehicles base their decisions more on the downstream, i.e., frontal, conditions than the upstream conditions. [13] summarize the second point in more detail based on Daganzo's requiem. They 'rename' this point as *Insufficient description of jam fronts* and provide several quotes of Daganzo. Here, it is noted that behavior at the end of the queue spreads for the back to the front, e.g., *new arrivals in the queue compress a queue from behind* and *vehicles at the end of the queue move back and this behavior spreads to the remaining vehicles in the queue*. The third point addresses the heterogeneous microscopic behavior. This heterogeneous behavior can be explained both based on the vehicle and driver characteristics. For instance, a truck and passenger car are expected to behave differently. [13] states that this problem can be addressed by using a multi-class model. However, this would not fully capture the behavioral heterogeneity of different drivers as two drivers using the same car may still have a heterogeneous behavior for the same traffic conditions.

In this conclusions, [3] states: *A new theory (e.g., relativity) is seemed successful if it explains previously unexplained phenomena, plus everything that was correctly explained with the theory it intends to replace (e.g., Newtonian physics).* Daganzo reasons that the new models is unable to capture behavior which is captured by the older and simpler LWR-model and therefore should not be considered as an improvement.

[1] and [13] believe [3] rejects the discussed second-order models for good reasons (although [1] use use quotation marks around the word *good*). However, in their view [3] Requiem does not relate to second-order models in general. The problems with the second-order model discussed by Daganzo can be overcome by improving the macroscopic traffic models. This view has led to the development (or improvement) of new second-order traffic flow models. According to [13], the most prominent example is the Aw-Rascle-Zhang (ARZ) model [1], [42]. In their work, [13] discuss the properties of this model. As this predominantly is a mathematical discuss, we will not discuss it here. If the reader is interested he/she is refereed to [13].

5

Method of Characteristics

Panchamy Krishnakumari

According to shockwave theory, the flow at capacity will have infinite acceleration, which is not realistic. There is another alternative to shockway theory that doesn't have this assumption based on the observation that, from the formula for density $\rho(x,t) = f(x - at)$, if we hold $x - at$ fixed then the solution is constant. In other words, if $x - at = x_0$ then $\rho = f(x_0)$ along this line as shown in figure 5.1. The observation that the solution is constant along the characteristics can be used to evaluate the solution anywhere in the x-t plane. These lines are called characteristics or kinematic waves.

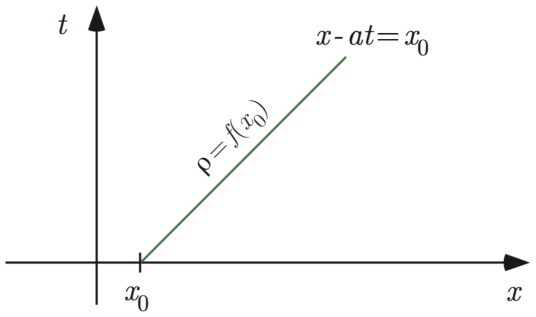

Figure 5.1: The characteristics are the straight lines $x - at = x_0$. Along each line the density is constant [15].

A kinematic wave can also be interpreted as a shockwave resulting from a sufficiently small change in state and the slope of the wave depends on the condition. The characteristic speed of a traffic state is the slope of the tangent at the given point on the fundamental diagram and the vehicle speed is the slope of the line between the origin and the given point as shown in Figure 5.2. This shows that the characteristic speed or kinematic speed at a given point along the fundamental diagram is either moving forward (free-flow) with the traffic stream or against (congestion) the traffic stream, if the traffic state is in the congestion branch.

Here, we will briefly explain how to construct the characteristic wave for a real world example. Consider a link on which there is a traffic flow in stationary equilibrium with constant density and this flow is suddenly brought to rest either through an accident or a traffic signal thus forming traffic queue upstream of the traffic light. The density distribution of this link is given in figure 5.3(b). The fan of kinematic waves (characteristics) corresponding to this situation is shown in figure 5.3(b).

The steps to construct this acceleration fan is as follows:

- Assume a fundamental diagram for the given link. Here, we make the traffic conditions continuous so that there is gradual change from one state to another and not an abrupt change(not a triangular fundamental diagram) as shown in figure 5.3(a).
- For each state in the fundamental diagram, estimate the characteristic speed by finding the tangent at the point as shown before. For example, for state with density $k_1 > k_c$, (critical density) the characteristic speed is shown in figure 5.3(a).

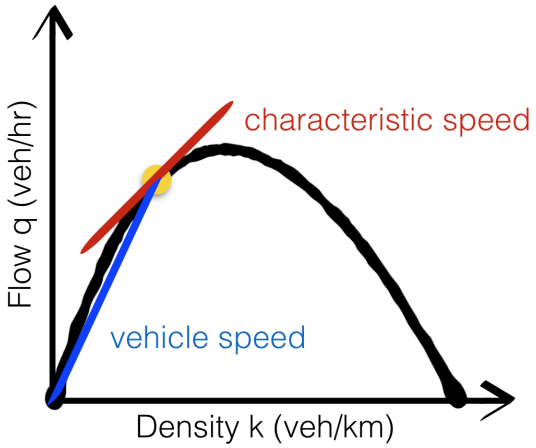

Figure 5.2: Vehicle speed and characteristic speed on the fundamental diagram

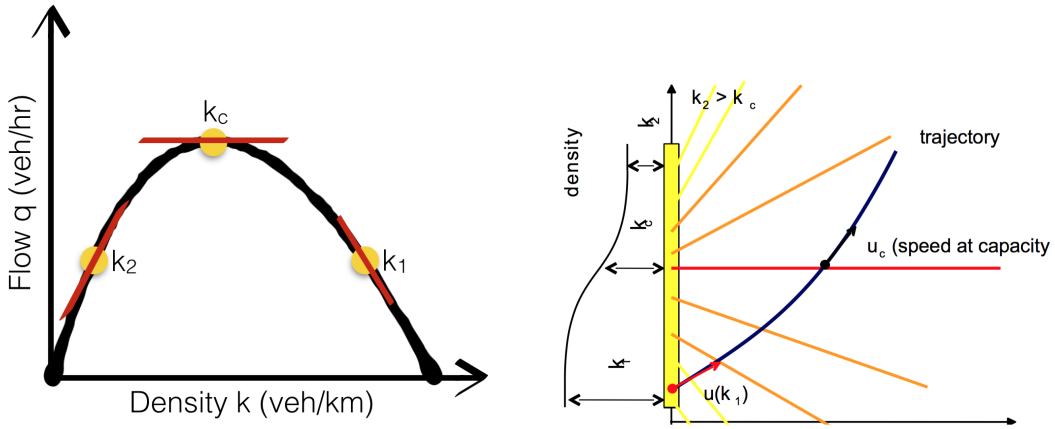

(a) Traffic states on the fundamental diagram

(b) Characteristic speeds [18]

Figure 5.3: Acceleration fan

- Propagating through the density distribution of the link, the characteristic wave for each state is found from the tangent of the corresponding state in the fundamental diagram, thus forming the acceleration fan as shown in figure 5.3(b).

Now, consider another real life situation where the traffic slows down due to a traffic light or opened bridge. The density distribution in such a case is shown in figure 5.4(b). The previous steps are used to construct the fan of kinematic waves, shown in figure 5.4(b), based on the fundamental diagram in figure 5.4(a). The deceleration fan obtained shows that the characteristics of the incoming traffic both before and after the blockage are interacting with each other. Thus for a given point, there are two values which is not plausible. Therefore, we revert to shockwave theory when the characteristics speed start interacting with each other.

Thus these steps can be used to construct the characteristic curves analytically for different real world scenarios.

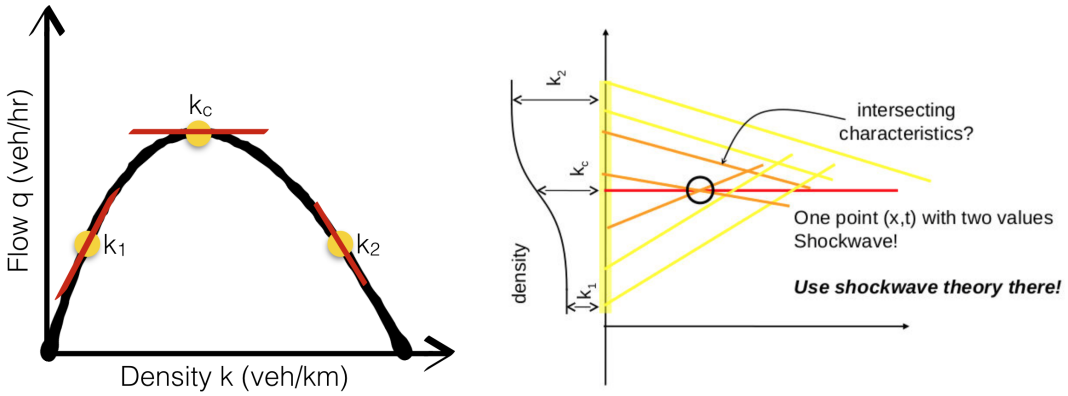

(a) Traffic states on the fundamental diagram

(b) Characteristic speeds [18]

Figure 5.4: Deceleration fan

6

Multi-class Modelling

Alexandra Gavriilidou

The original kinematic wave theory model (LWR model) assumes that traffic is homogeneous and is, thus, called single- or mixed-class. This model has been extended to account for heterogeneity in traffic and the corresponding models are referred to as multi-class models. The multi-class models have been found to be able to reproduce traffic phenomena such as the two-capacity (or reverse-lambda) regimes in the fundamental diagram, hysteresis and platoon dispersion [2, 4, 31, 34, 40]. Therefore, it is worth discussing them.

According to Logghe and Immers [27], the modelling of heterogeneous properties can be allocated either to the infrastructure or to the vehicles and drivers. The first approach makes a distinction between lanes and formulates a separate LWR model for each lane, each with a separate fundamental diagram. These parallel models communicate via exchange terms which depend on the driving conditions on the lanes [14, 22, 28, 29]. The second approach, which is the most popular, subdivides the vehicle flow into classes which share the same properties. The heterogeneity is, then, the result of interactions between these homogeneous subgroups.

As with single-class models, multi-class models can be formulated in Eulerian or Lagrangian coordinates. The former is based on the conservation of vehicles law, which is applied to each class as well as to the overall traffic. In Lagrangian coordinates two formulations exist, based on whether the vehicle number is defined over all classes or differs per class. These models are discussed in sections 6.1 and 6.2, respectively.

6.1. Eulerian coordinates

Logghe and Immers [27] reviewed existing multi-class LWR models in Eulerian coordinates and proposed a framework whereby these models are interpreted as an assignment of road space to classes. Each class is assigned to a fraction of road space and based on the way this assignment is made, seven types of models are distinguished:

1. Multi-commodity classes: correspond to each OD-relation in a network and have the same fundamental diagram
2. Special lanes: accessible only to a specific class, classes have the same fundamental diagram
3. Equal space: all vehicles have the same gross space headway
4. Equal distance gap: all vehicles have the same net space headway
5. Distance gap proportional to vehicle length: headway is not determined by speed, but by vehicle length
6. Equal speed: in congestion all classes have the same speed
7. User-equilibrium: non-cooperative interaction, where all vehicles seek to maximise their speed

A common denominator for these models is that they rescale the fundamental relation [37]. A different approach was used by Van Lint et al. [35], where the effective density is computed and used as input for the fundamental relation. This is because all vehicles experience the combined/global density but the way they react to it is

class-specific. The effective density k_{tot} is a weighted summation of the class-specific densities k_u with respect to the passenger car equivalent (PCE: η) values:

$$k_{\text{tot}} = \sum_u \eta_u k_u \tag{6.1}$$

where the subscript u is a class-specific index.

The PCE values can be either constant (dependent on the geometry (slope, grade, curvature), vehicle characteristics, truck percentage) or dynamic (state-dependent). In the latter case, they can be dynamically calculated by:

$$\eta_u = \frac{L_u + T_u V_u(k_{\text{tot}})}{L_{\text{car}} + T_{\text{car}} V_{\text{car}}(k_{\text{tot}})} \tag{6.2}$$

where L_u denotes the class-specific gross stopping distance (average vehicle length), T_u denotes the class-specific reaction time (minimum time headway) and $V_u(k_{\text{tot}})$ is the class-specific fundamental relation ($v - k$).

This dynamic PCE value formulation takes into account the prevailing traffic conditions (through the speeds) and captures the ratio of the effective-occupied road lengths between one class-u vehicle and one passenger car, i.e. a truck takes relatively more space, when compared to a car, in congestion than under free-flow conditions.

Last but not least, Nair et al. [30] developed the porous flow model for disordered traffic flow with different types of vehicles such as cars, scooters and bikes and without lanes. According to this model, small vehicles can drive through "pores", i.e. openings between other vehicles [37].

6.2. Lagrangian coordinates

As already mentioned, there are two model formulations in Lagrangian coordinates, namely the "Piggy-back" model, which is based on one coordinate system, and the "Multi-pipe" model which is based on several independent coordinate systems for each of the vehicle classes. The subsections below provide a summary of these models, while the reader is referred to [41] for more details.

6.2.1. "Piggy-back" model

In this model, there is one main class and one that is described relative to it. In [36], the derivation is partly based on the single-class Lagrangian conservation equation for the reference class:

$$\frac{\mathrm{D}s_1}{\mathrm{D}t} + \frac{\partial v_1}{\partial n} = 0 \tag{6.3}$$

and partly based on the conservation of vehicles law for the other classes:

$$\frac{\mathrm{D}s_u}{\mathrm{D}t} + \frac{s_u}{s_1}\frac{\partial v_u}{\partial n} + \frac{v_1 - v_u}{s_1}\frac{\partial s_u}{\partial n} = 0 \tag{6.4}$$

where $\frac{\mathrm{D}}{\mathrm{D}t} = \frac{\partial}{\partial t} + v_1 \frac{\partial}{\partial x}$ is the Lagrangian derivative.

In this formulation, n denotes the vehicle/platoon number of class 1, while the numbering for vehicles of other classes does not have actual meanings. The vehicles from other classes are essentially travelling along with platoons of class 1, which leads to the name "Piggyback" (i.e. each platoon of class 1 carries with it a certain number of other class vehicles while traversing over the network). Figure 6.1 illustrates the vehicle discretisation in this formulation at a time instant.

A class-specific fundamental relation is used and the effective vehicle spacing s_{tot} is computed by:

$$s_{\text{tot}} = \frac{1}{\sum_u \eta_u / s_u} \tag{6.5}$$

where the subscript u is a class-specific index.

The equation 6.6 then becomes:

$$\eta_u = \frac{L_u + T_u V_u(s_{tot})}{L_{\text{car}} + T_{\text{car}} V_{\text{car}}(s_{\text{tot}})} \tag{6.6}$$

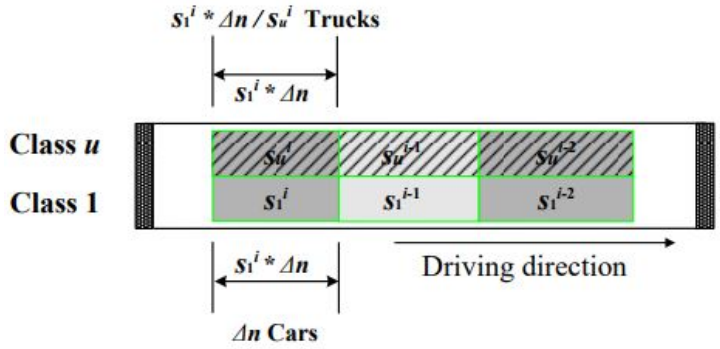

Figure 6.1: Vehicle discretisation at a time instant in the "Piggy-back" formulation (two class case). The rectangular cell denotes vehicle platoon of size Δn [41].

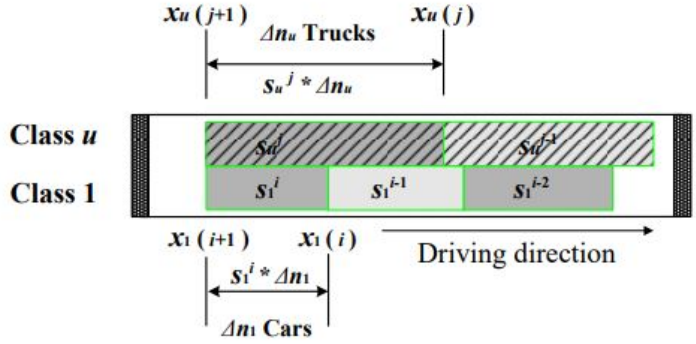

Figure 6.2: Vehicle discretisation at a time instant in the "Multi-pipe" formulation (two class case). i and j denote the indices respectively for class 1 (passenger cars) and class u (trucks) [41].

.

6.2.2. "Multi-pipe" model

This model can be directly derived from the single-class Lagrangian conservation equation which holds for each class u and indicates that the change of vehicle spacing over time should be equal to the change of vehicle speed over vehicle number in each class:

$$\frac{\mathrm{D}s_u}{\mathrm{D}t} + \frac{\partial v_u}{\partial n_u} = 0 \tag{6.7}$$

where $\frac{\mathrm{D}}{\mathrm{D}t} = \frac{\partial}{\partial t} + v_u \frac{\partial}{\partial x}$ is the Lagrangian derivative. n_u denotes the vehicle number of user class u.

Similar to the "Piggy-back" model, each class has its own fundamental relation and the effective spacing is the link between the different classes 6.5. The main difference from the "Piggy-back" formulation is that an independent coordinate system is introduced for each of the classes. This means that vehicles from each class are clustered in platoons and numbered separately. Consequently, the platoon size for each class Δn_u can be chosen differently. According to the conservation law, the class-specific platoons only react to the consecutive same-class platoons via the equilibrium speed. This equilibrium speed, however, is a function of the effective vehicle spacing. Figure 6.2 illustrates the related vehicle discretisation at a time instant.

6.2.3. Comparison

In terms of application of the two formulations, the "Piggy-back" model is suitable for real-time applications, such as traffic state estimation and prediction. This is because the single coordinate system makes it very computationally efficient. In contrast, in the "Multi-pipe" model, the coordinate systems are as many as the classes, which is a more intuitive and understandable way to represent class-specific traffic. However, the calculation of the equilibrium speed requires an additional interaction term, which increases the computational time and complexity.

Despite this advantage of the "Piggy-back" model, it should be kept in mind that it is formulated based only on class 1. This may lead to problems if the density of this class is small compared to the others. In this case, large numerical errors may be introduced, and the total vehicle number of the other classes that are carried by the

Table 6.1: Comparison between two formulations of the multi-class Lagrangian model [41].

	"Piggy-back" formulation	"Multi-pipe" formulation
Real-time applications	+	-
Suitability for state estimation models	+	-
Suitability for incorporating network discontinuities	-	+
Class-specific control and OD estimations	-	+

first-class platoons might change rapidly. The "Multi-pipe" model might, therefore, be more appropriate. This leads to a trade-off between the ease of implementation and the simulation accuracy.

Another advantage of the "Multi-pipe" model is its suitability for network discontinuities (e.g. on-ramps) and class-specific modelling (control applications and OD estimations). The main benefit comes from the fact that the in-flow of each class is dealt with separately. However, the application of the "Multi-pipe" formulation in traffic state estimation is considerably more complex, thereby limiting its applicability.

An overview of these advantages and disadvantages is given in table 6.1.

7

Macroscopic Fundamental Diagram

Panchamy Krishnakumari

When the variables of flow, speed and density are estimated as average values at a road network-level, then these are defined as its macroscopic characteristics and the relationships that arise between them are named Macroscopic Fundamental Diagrams (MFD), in contrast to the Fundamental Diagrams (FD) that refer to specific road sections. The existence of MFD was initially reported in Geroliminis and Daganzo [11] as shown in figure 7.1. From the figure, it is evident that the individual detections provides no evident relationship whereas the average of these variables start exhibiting correlations. The MFD variables are named as accumulation (average density), production (average internal flow) and performance (outflow).

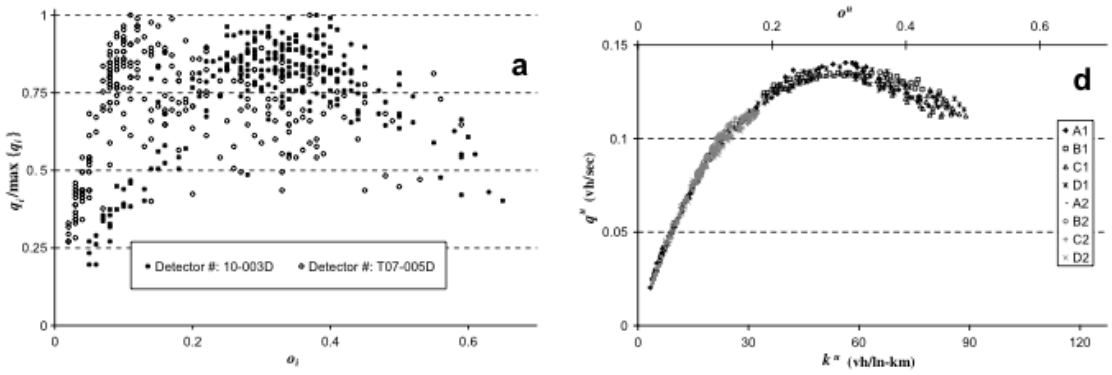

Figure 7.1: Loop detector data from Yokohama (Japan) (a) flow vs. occupancy pairs for two single detectors across a day; (d) average flow vs. average occupancy from all the detectors across two different days [11]

7.1. Network Fundamental Diagram

There are different levels for traffic management as shown in figure 7.2. The commonly used microscopic which is vehicle level and macroscopic is link level. These levels are sufficient to simulate small sections. However, in the cities congestion spreads in different direction and the whole city need to be described. This requires another way of describing. Thus a new zone level or sub-network level was described based on the existence of a macroscopic fundamental diagram. The idea was that each of the sub-network will have an MFD associated with it. Literature loosely term it as network fundamental diagram (NFD) even though it is the same as MFD. The Network fundamental diagram describes the relationship between accumulation (average density) and the (unrestricted) outflow out of the network.

7.2. Network Transmission Model

The Network Fundamental Diagram (NFD) describes the relation between flow and density on a network level. A traffic model which uses this relationship, representing traffic and traffic dynamics at a high spatial scale is

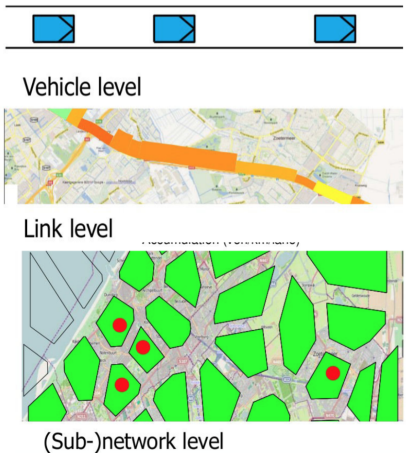

Figure 7.2: Different scales - vehicle level, link level and zone level [21]

a network transmission model (NTM) and was introduced in Knoop and Hoogendoorn [21]. Larger areas need a longer time horizon for the traffic optimization and using such sub-network based approaches can make it faster. The supply and demand for the NTM are based on the NFD. The demand is the same as the NFD for all densities. This is contrary to the cell transmission model where demand stays high for overcritical situations. However, in networks, gridlocks can occur. The supply for NTM at under critical accumulation is similar to the cell transmission model at capacity and follows the NFD for higher accumulations. The supply and demand characteristics used for NTM are shown in figure 7.3.

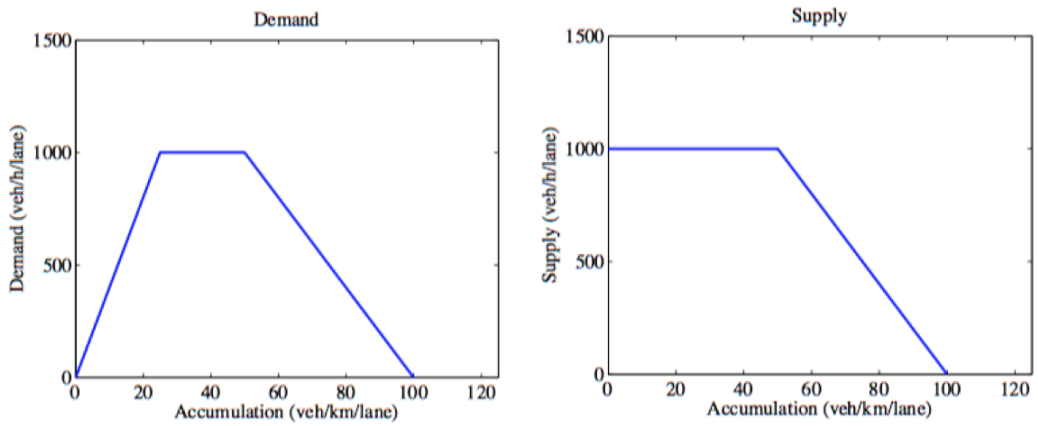

Figure 7.3: Demand and Supply Characteristics of NTM [21]

8

Active Modes

Alexandra Gavriilidou This chapter defines the traffic flow variables for multi-directional movements and presents models for active mode traffic.

8.1. Multi-directional variables (presentation Dorine Duives)

Even though research in active mode traffic is still fairly young and the dimensionality of the problem raises new questions with respect to definitions, it is worth looking at the ways that the main traffic flow variables are being defined for pedestrian traffic.

Since the movement of a pedestrian takes place in two dimensions, the walking speed has a magnitude as well as a direction in space. This leads to three types for the definition of speed, namely (i) velocity, which corresponds to the vector v_x, v_y; (ii) absolute speed, which is the magnitude of the vector, and (iii) effective speed, which is v_x, while v_y can be seen as an indicator for the stability ("temperature") of the total flow. The absolute speed is the one use more often, but it has not yet been answered which of the types of speed should be used.

With respect to the definition of density, many options have been proposed and four of them are presented and visualised in 8.1:

1. Grid-based assessment: counts persons within (even partially) each cell
2. Adapted grid-based: each person is in the centre of his/her cell
3. Adapted XT-method: takes into account a time/space cell
4. Voronoi: area belonging to each person, which makes it challenging to go macroscopic from each cell density

The grid-based assessment is often used or Voronoi's density in order to limit computational efforts.

However, a quantification of density does not automatically represent how pedestrians experience that density. To this end, the level of service (LOS) has been defined, representing the experienced density. Fruin (1971) used the amount of space that was allotted to a pedestrian as a measure for LOS and an illustration can be seen in figure 8.2. It is important, however, to note that the time spent in each LOS is what really matters, since pedestrians might be willing to accept a very low LOS for a short period of time (e.g. when alighting from a bus).

Regarding the definition of flow, it is currently defined at a cross-section similar to car traffic. However, the multi-directionality of the flows raises questions with respect to the aggregation method. If the flows are simply added, it might result in negative flows, while other approaches would be to add partial vectors of flow or just the absolute values. A contemporary solution is either to determine two flows (in and out) at each cross-section or to account for the total flow.

An overview of the units used for pedestrian as opposed to car traffic is given in table 8.1.

A sketch of the fundamental diagram for pedestrian traffic can be seen in figure 8.3. Assuming that the black line represent the general form, the effect of different factors is shown with the arrows and the shifted (coloured) lines. The red line corresponds to tired pedestrians, while the blue one to pedestrians that are in a rush. Last but not least, the green line represents crowd mindedness (i.e. self-organisation phenomena). An idea to incorporate the pedestrian heterogeneity (e.g. elderly, children, tourists) would be to define a concept similar to the PCE (for example healthy-young-male equivalents).

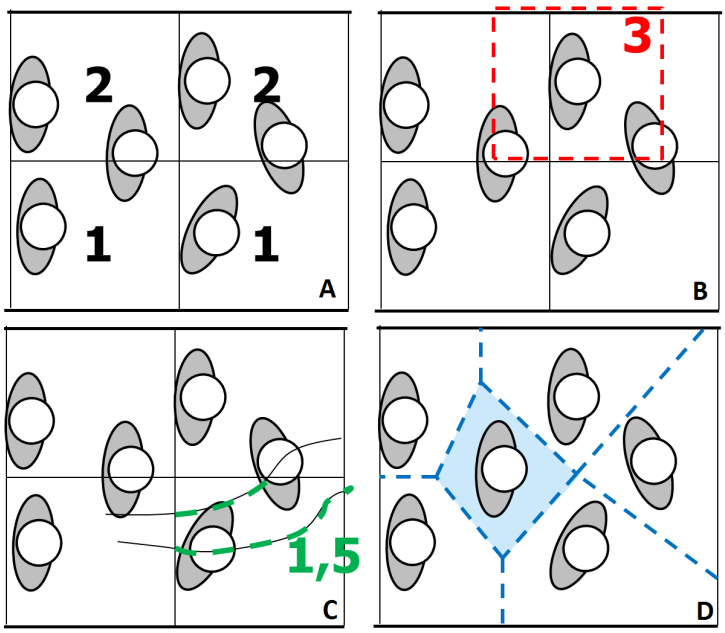

Figure 8.1: Pedestrian density based on: A: grid-based assignment; B: adapted grid-based; C: Adapted XT-method and D: Voronoi

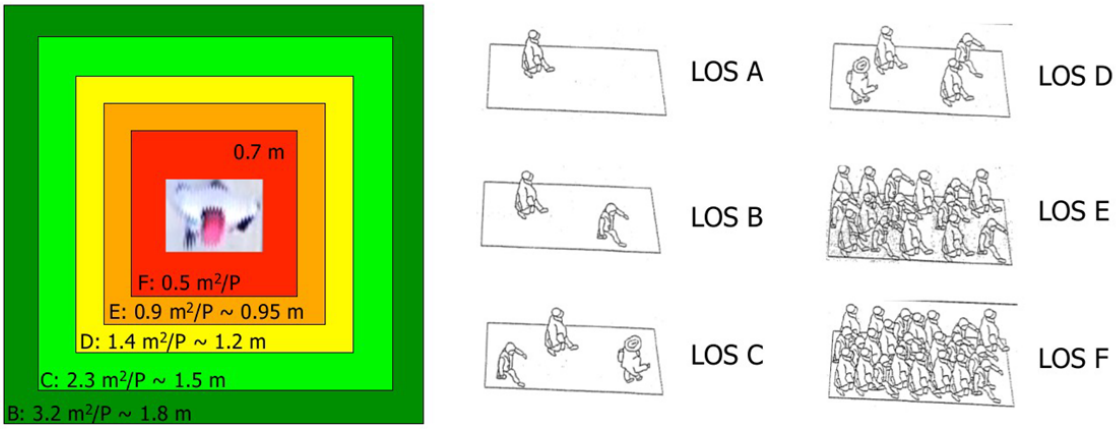

Figure 8.2: Illustration of proposed walkway Level of Service thresholds, adapted from [10].

Table 8.1: Traffic flow variable units.

Variable	Car traffic	Pedestrian traffic
Speed	km/h	m/s
Density	veh/km	ped/m^2
Flow	veh/h	ped/m/s

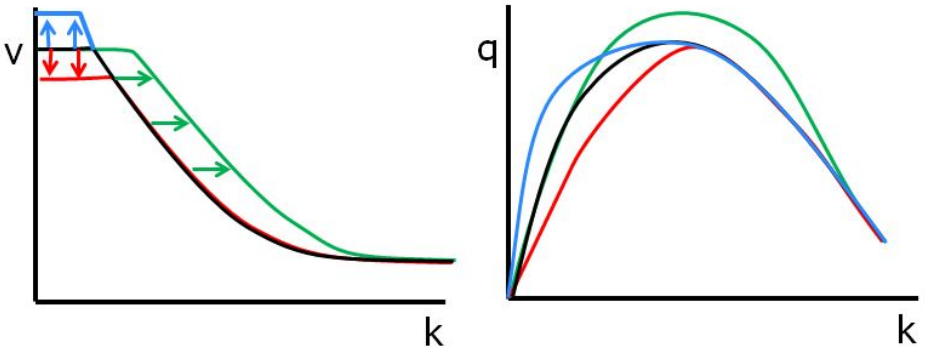

Figure 8.3: Sketches of the fundamental diagram for pedestrian traffic.

Table 8.2: Traffic characteristics per mode.

	Cars	Cyclists	Pedestrians
Directionality	Uni-directional	Depending on infrastructure	Multi-directional
Flow conservation	Yes	No	No
Interactions	1D	1D or 2D	2D
Contact	No	No	Possible
Travel time	Optimised	Depending	Depending
OD restrictions	Yes	Sometimes	No
Anisotropy	Strong	Medium	Mild

8.2. Modelling active mode traffic (presentation Marie-Jette Wierbos)

Except for the multi-directionality, active mode traffic differs from motorised traffic in several aspects. Examples are the lack of lanes, the multi-dimensional interactions and the fact that they are less regulated by traffic rules. Table 8.2 shows several traffic characteristics for cars, cyclists and pedestrians.

In the modelling of pedestrian flows, behavioural rules are taken into account. They reflect the fact that pedestrians head towards a specific target and aim to keep their direction, while being attracted and repelled from road users and the infrastructure around them. Additionally, the visual and sensory fields of pedestrians determine their perception of space and their surroundings. In situation where panic prevails, a bump can be observed in the fundamental, increasing the jam density (k_j to $k*_j$) (figure 8.4).

As already mentioned, another characteristic of pedestrian flows is that it is self-organised, i.e. coordinated spatial distribution arises by 1-to-1 interaction of individuals or by applying local behavioural rules. Some examples of self-organisation are:

- Arching at bottlenecks (e.g. around a door)
- Lane formation in crossing flows
- V-like, River-like and Wall-like configurations

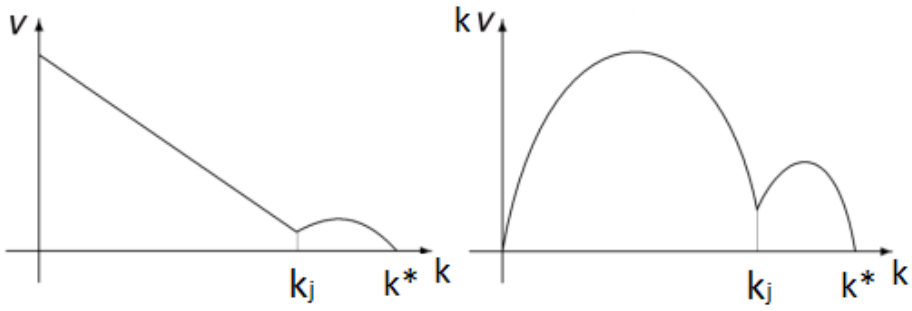

Figure 8.4: Fundamental diagram in case of panic within the crowd of pedestrians.

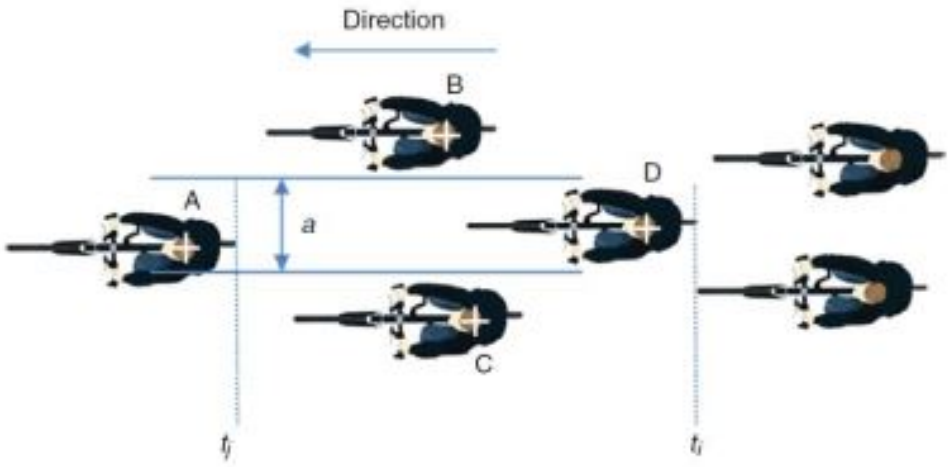

Figure 8.5: Headway definition using the width a as the key decision variable to determine which cyclist is being followed. In the figure, cyclist D is following cyclist A [16].

- Herding and Zipper effect (i.e. temporarily allow people to zip into their personal space)

With respect to the modelling of cyclists, their behavioural rules lie somewhere in between those of cars and pedestrians. Hoogendoorn and Daamen [16] developed a bicycle headway model which considers two traffic states, free flow and congested, similar to leader-follower in cars. The desired free space (i.e. minimum headway) fluctuates and this heterogeneity is attributed to the perception of safety and comfort, as well as the skills and cycling purpose. Figure 8.5 shows how the bicycle headway was defined.

Another approach that could be used to model cyclists macroscopically is the porous system developed by Nair et al. [30]. An empirical study in Chinese bicycle paths where a lane drop exists derived the fundamental diagram for cyclists [25]. According to that, the average speed decreases as the density increases. Also, the amount of overtaking increases with density but decreases in congested traffic conditions. The empirical study showed that even when rhe average speed was quite low, bicycle traffic could still maintain a relatively large flow, which is different from the results in simulation studies. It is obvious that more research is required in this field.

Bibliography

[1] a Aw and Michel Rascle. Resurrection of" second order" models of traffic flow. *SIAM journal on applied mathematics*, 60(3):916–938, 2000.

[2] Nicola Bellomo and Christian Dogbe. On the modeling of traffic and crowds: A survey of models, speculations, and perspectives. *SIAM review*, 53(3):409–463, 2011.

[3] Carlos F Daganzo. Requiem for second-order fluid approximations of traffic flow. *Transportation Research Part B: Methodological*, 29(4):277–286, 1995.

[4] Carlos F Daganzo. A behavioral theory of multi-lane traffic flow. part i: Long homogeneous freeway sections. *Transportation Research Part B: Methodological*, 36(2):131–158, 2002.

[5] Carlos F. Daganzo. A variational formulation of kinematic waves: basic theory and complex boundary conditions. *Transportation Research Part B*, 2005.

[6] Carlos F. Daganzo. A variational formulation of kinematic waves: Solution methods. *Transportation Research Part B*, 2005.

[7] Carlos F. Daganzo and Nikolas Geroliminis. An analytical approximation for the macroscopic fundamental diagram of urban traffic. *Transportation Research Part B*, 2008.

[8] Carlos F. Daganzo and Victor L. Knoop. Traffic flow on pedestrianized streets. *Transportation Research Part B*, 2016.

[9] Lawrence C. Evans. *Partial Differential Equations*. American Mathematical Society Providence, Rhode Island, 2nd edition edition, 2010.

[10] John J Fruin. *Pedestrian planning and design*. New York : Metropolitan Association of Urban Designers and Environmental Planners, 1971. Based on the author's thesis, originally presented at the Polytechnic Institute of Brooklyn under the title: Designing for pedestrians.

[11] Nikolas Geroliminis and Carlos F Daganzo. Existence of urban-scale macroscopic fundamental diagrams: Some experimental findings. *Transportation Research Part B: Methodological*, 42(9):759–770, 2008.

[12] Sergei Konstantinovich Godunov. A difference method for numerical calculation of discontinuous solutions of the equations of hydrodynamics. *Matematicheskii Sbornik*, 89(3):271–306, 1959.

[13] Dirk Helbing and Anders Johansson. On the Controversy around Daganzo ' s Requiem for and Aw-Rascle ' s Resurrection of Second-Order Traffic Flow Models. *The European Physical Journal B*, 69(4):549–562, 2009.

[14] Edward N Holland and Andrew W Woods. A continuum model for the dispersion of traffic on two-lane roads. *Transportation Research Part B: Methodological*, 31(6):473–485, 1997.

[15] M.H. Holmes. Characteristics line. `http://pub.math.leidenuniv.nl/~chirilusbrucknerm/ds_seminar_2016/holmes_Ch5_traffic_flow.pdf`, 2016.

[16] Serge Hoogendoorn and Winnie Daamen. Bicycle headway modeling and its applications. *Transportation Research Record: Journal of the Transportation Research Board*, (2587):34–40, 2016.

[17] W L Jin and H M Zhang. Solving the Payne-Whitham traffic flow model as a hyperbolic system of conservation laws with relaxation. Technical report, University of California, Davis, 2001.

[18] Victor Knoop. Acceleration and deceleration. `https://ocw.tudelft.nl/wp-content/uploads/6._Traffic_analysis__characteristics.pdf`, 2014.

[19] Victor L. Knoop. *Introduction to Traffic Flow Theory: An introduction with exercises*. 2017.

[20] Victor L. Knoop. Macroscopic traffic modelling. Lecture slides, Delft University of Technology, 2017.

[21] Victor L Knoop and Serge P Hoogendoorn. Network transmission model: a dynamic traffic model at network level. In *Transportation Research Board 93rd Annual Meeting*, number 14-1104, 2014.

[22] Jorge A Laval and Carlos F Daganzo. Multi-lane hybrid traffic flow model: a theory on the impacts of lane-changing maneuvers. In *84th transportation research board's annual meeting, Washington, DC*, 2005.

[23] Jorge A Laval and Ludovic Leclercq. The hamilton–jacobi partial differential equation and the three representations of traffic flow. *Transportation Research Part B: Methodological*, 52:17–30, 2013.

[24] Ludovic Leclercq, Jorge Andres Laval, and Estelle Chevallier. The lagrangian coordinates and what it means for first order traffic flow models. In *Transportation and Traffic Theory 2007. Papers Selected for Presentation at ISTTT17*, 2007.

[25] Zhibin Li, Mao Ye, Zheng Li, and Muqing Du. Some operational features in bicycle traffic flow: Observational study. *Transportation Research Record: Journal of the Transportation Research Board*, (2520):18–24, 2015.

[26] M. J. Lighthill and G. B. Whitham. On Kinematic Waves. II. A Theory of Traffic Flow on Long Crowded Roads. *Proceedings of the Royal Society A: Mathematical, Physical and Engineering Sciences*, 229(1178): 317–345, may 1955. ISSN 1364-5021.

[27] S Logghe and Lambertus H Immers. Multi-class kinematic wave theory of traffic flow. *Transportation Research Part B: Methodological*, 42(6):523–541, 2008.

[28] PK Munjal and Louis Albert Pipes. Propagation of on-ramp density perturbations on unidirectional two-and three-lane freeways. *Transportation Research*, 5(4):241–255, 1971.

[29] PK Munjal, Yuan-Shih Hsu, and RL Lawrence. Analysis and validation of lane-drop effects on multi-lane freeways. *Transportation Research*, 5(4):257–266, 1971.

[30] Rahul Nair, Hani S Mahmassani, and Elise Miller-Hooks. A porous flow model for disordered heterogeneous traffic streams. In *Transportation Research Board 91st Annual Meeting*, number 12-3260, 2012.

[31] D Ngoduy. Multiclass first-order traffic model using stochastic fundamental diagrams. *Transportmetrica*, 7 (2):111–125, 2011.

[32] Harold J. Payne. Models of Freeway Traffic and Control. In *Mathematical Models of Public Systems, La Jolla, California Simulation Councils*, volume 1, pages 51–61, 1971.

[33] Paul I . Richards. Shock Waves on the Highway. *Operations Research*, 4(1):42–51, 1956.

[34] Martin Treiber and Dirk Helbing. Macroscopic simulation of widely scattered synchronized traffic states. *Journal of Physics A: Mathematical and General*, 32(1):L17, 1999. URL `http://stacks.iop.org/0305-4470/32/i=1/a=003`.

[35] J Van Lint, Serge Hoogendoorn, and Marco Schreuder. Fastlane: New multiclass first-order traffic flow model. *Transportation Research Record: Journal of the Transportation Research Board*, (2088):177–187, 2008.

[36] Femke van Wageningen-Kessels, Yufei Yuan, Serge P Hoogendoorn, Hans Van Lint, and Kees Vuik. Discontinuities in the lagrangian formulation of the kinematic wave model. *Transportation Research Part C: Emerging Technologies*, 34:148–161, 2013.

[37] Femke van Wageningen-Kessels, Hans Van Lint, Kees Vuik, and Serge Hoogendoorn. Genealogy of traffic flow models. *EURO Journal on Transportation and Logistics*, 4(4):445–473, 2015.

[38] John Glen Wardrop. Some Theoretical Aspects of Road Traffic Research. *Road engineering division meeting*, pages 325–362, 1952.

[39] G. B. Whitham. *Linear and non-linear waves*. 1974. ISBN 0471940909.

[40] GCK Wong and SC Wong. A multi-class traffic flow model–an extension of lwr model with heterogeneous drivers. *Transportation Research Part A: Policy and Practice*, 36(9):827–841, 2002.

[41] Yufei Yuan. Lagrangian multi-class traffic state estimation. 2013.

[42] H.M. Zhang. A non-equilibrium traffic model devoid of gas-like behavior. *Transportation Research Part B: Methodological*, 36(3):275–290, 2002. ISSN 01912615.